Molecular Pharmacology Fast Forward. Published on August 9, 2010 as doi:10.1124/mol.110.067199
This article has not been copyedited and formatted. The final version may differ from this version.

PARP1 modulates the lethality CHK1 inhibitors in carcinoma cells.

Clint Mitchell, Margaret Park, Patrick Eulitt, Chen Yang, Adly Yacoub and Paul Dent*

Department of Neurosurgery, Virginia Commonwealth University, 401 College St., Richmond, VA 23298.

Molecular Pharmacology Fast Forward. Published on August 9, 2010 as DOI: 10.1124/mol.110.067199
This article has not been copyedited and formatted. The final version may differ from this version.

Running Title:
PARP1 and CHK1

Document statistics:
Text pages: 29
Tables: 2
Figures: 5
References: 38
Words in abstract: 221
Words in introduction: 692
Words in discussion: 1022

Abbreviations: ERK: ex tracellular r egulated k inase; MEK : m itogen act ivated e xtracellular r egulated kinase; PARP: poly (ADP-ribose) polymerase.

*Correspondence to:
Paul Dent, Ph.D.
Department of Neurosurgery
Box 980035
Virginia Commonwealth University
Richmond VA 23298-0035.
Tel: 804 628 0861
Fax: 804 827 1014
pdent@vcu.edu

Molecular Pharmacology Fast Forward. Published on August 9, 2010 as DOI: 10.1124/mol.110.067199
This article has not been copyedited and formatted. The final version may differ from this version.

Abstract.

Prior studies have demonstrated that inhibition of CHK1 can promote activation of ERK1/2 and phosphorylation of histone H2AX, and also that inhibition of PARP1 can impact on growth factor –induced ERK1/2 activation. The present studies were initiated to determine in whether CHK1 inhibitors interacted with PARP1 inhibition to facilitate apoptosis. Transient expression of dominant negative CHK1 raised basal ERK1/2 activity and prevented CHK1 inhibitors from activating ERK1/2. CHK1 inhibitors modestly increased the levels of PARP1 ADP ribosylation and molecular or small molecule inhibition of PARP1 blocked CHK1 inhibitor –stimulated histone H2AX phosphorylation and activation of ERK1/2. Stimulated histone H2AX phosphorylation was ATM dependent. Multiple CHK1 inhibitors interacted in a greater than additive fashion with multiple PARP1 inhibitors to cause transformed cell killing in short term viability assays and synergistically killed tumor cells in colony formation assays. Over-expression of BCL-XL or loss of BAX/BAK function, but not the function of BID, suppressed CHK1 inhibitor + PARP1 inhibitor lethality. Inhibition of BCL-2 family protein function enhanced CHK1 inhibitor + PARP1 inhibitor lethality and restored drug-induced cell killing in cells over-expressing BCL-XL. Thus PARP1 plays an important role in regulating the ability of CHK1 inhibitors to activate ERK1/2 as well as the DNA damage response. An inability of PARP1 to modulate this response results in transformed cell death mediated through the intrinsic apoptosis pathway.

Molecular Pharmacology Fast Forward. Published on August 9, 2010 as DOI: 10.1124/mol.110.067199
This article has not been copyedited and formatted. The final version may differ from this version.

Introduction.

Multiple CHK1 inhibitors including UCN-01 (7-hydroxystaurosporine) and AZD7762 are currently being evaluated as anti-neoplastic agents in clinical trials, both alone and in combination with chemotherapeutic agents and ionizing radiation (Mow et al, 2001; Prudhomme, 2006). These agents are proposed to enhance the toxicity of chemotherapeutic drugs by inhibition of CHK1 with subsequent inappropriate cell cycle progression after DNA damage (Graves et al, 2000). Inhibition of CHK1 may directly promote activation of the protein phosphatase CDC25C and can also interfere with CDC25C elimination by blocking its binding to 14-3-3 proteins and subsequent degradation (Graves et al, 2000; Peng et al, 1997). The CHK1 inhibitor UCN-01 is known to have many additional intracellular kinase targets including the downstream effector of PI3 kinase, PDK-1, as well as "classical" PKC isoforms (Komander et al, 2003).

Based on initial phase I studies, the maximal free achievable concentration of UCN-01 in human plasma was thought to be at or below ~100 nM with a long plasma half-life due to UCN-01 binding to human alpha 1 acidic glycoprotein (Sausville et al, 1998; Fuse et al, 1998; Hagenauer et al, 2004; Fuse et al, 2005; Dees et al, 2005). Nonetheless, the combination of UCN-01 with topotecan or cisplatin has shown some preliminary evidence of patient activity (Hotte et al, 2006; Perez et al, 2006). We have noted in a wide variety of tumor cell types that UCN-01 activates the ERK1/2 pathway, and that pharmacologic or genetic inhibition of the ERK1/2 pathway dramatically potentiates apoptosis and suppresses tumor growth in vivo (Dai et al, 2001; Dai et al, 2002; McKinstry et al, 2002; Hawkins et al, Hamed et al, 2008; Dai et al, 2008). Recently, we reported that the novel CHK1 inhibitor AZD7762 interacts with MEK1/2 inhibitors and farnesyltransferase inhibitors in a similar manner to UCN-01 to kill malignant hematopoietic cells in vitro (Pei et al, 2008). Thus multiple CHK1 inhibitors can interact with multiple MEK1/2 inhibitors to promote tumor cell killing. It has been noted that CHK1 inhibition leads to formation of single-and double-stranded DNA breaks, as judged by increased phosphorylation of the atypical histone H2AX, often referred to as γH2AX (Bucher and Britten, 2008; Syljuasen et al, 2005). Subsequently, we also noted that UCN-01, in addition to activating ERK1/2, promotes increased

Molecular Pharmacology Fast Forward. Published on August 9, 2010 as DOI: 10.1124/mol.110.067199
This article has not been copyedited and formatted. The final version may differ from this version.

phosphorylation of histone H2AX, indicative that DNA damage was occurring due to the inhibition of CHK1 function, and that inhibition of ERK1/2 further enhanced histone H2AX phosphorylation prior to induction of apoptosis (Dai et al, 2008). Thus CHK1 dependent regulation of ERK1/2 may play an important role DNA damage sensing and repair in transformed cells.

Cells contain multiple complexes of proteins that regulate DNA damage sensing and repair responses. One central protein in the regulation of multiple forms of DNA repair processes is poly (ADP-ribose) polymerase (PARP1), which due to its central role in DNA repair, particularly non-homologous end joining, and has been pharmacologically targeted for cancer therapeutics with inhibitors that block its ADP ribosylation and repair function (Schreiber et al, 2006; Schreiber et al, 2002; Rodon et al, 2009). Indeed, multiple PARP1 inhibitors have been developed with several in clinical use including GPI15427, CEP6800, NU1025 and AZD2281 (Grazia-Graziani and Szabo, 2005). Although initially noted for its role in the repair of DNA strand-breaks, PARP1 has been shown to have a much wider range of biologic actions and participates in the regulation of transcription, DNA replication, apoptosis, and modulating ROS levels (Quenet et al, 2009; McCabe et al, 2006; Spina-Purrello et al, 2002). We and others have noted that signaling from the EGF receptor can regulate PARP1 activity, in part through regulation of the ERK1/2 pathway (Hagan et al, 2007).

Based on the fact that CHK1 inhibitors activate ERK1/2 and promote H2AX phosphorylation, and that PARP1 function has been linked to ERK1/2 signaling, we investigated whether inhibition of PARP1 function modulated the activation of cell signaling pathways induced by CHK1 inhibitor treatment. Our data demonstrate that CHK1-induced phosphorylation of ERK1/2 and H2AX is blunted or abolished when PARP1 function or expression is reduced. A reduced ability of cells to increase ERK1/2 activation correlated with a synergistic induction of cell killing that was mediated through the intrinsic apoptosis pathway.

Molecular Pharmacology Fast Forward. Published on August 9, 2010 as DOI: 10.1124/mol.110.067199
This article has not been copyedited and formatted. The final version may differ from this version.

Materials and Methods.

Materials. Phospho-/total-ERK1/2 antibodies, GAPDH, 10H ADP ribosylation, PARP1, Phospho-/total-CHK1, ATM and Phospho-/total-H2AX antibodies were all purchased from Cell Signaling Technologies (Worcester, MA, USA). TUNEL kits were purchased from NEN Life Science Products (NEN Life Science Products, Boston, MA) and Boehringer Mannheim (Manheim, Germany), respectively. Trypsin-EDTA, RPMI, penicillin-streptomycin were purchased from GIBCOBRL (GIBCOBRL Life Technologies, Grand Island, NY). MDA-MB-231, MCF7, SKBR3, BT474 and PANC1 cells were purchased from the ATCC. The 4T1 line was kindly provided by Dr. A. Larner (VCU). SV40 Large T mouse embryonic fibroblasts lacking expression of various pro-apoptotic BH3 domain proteins were kindly provided by Dr. S. Korsmeyer (Harvard University, Boston, MA). The plasmid to express dominant negative CHK1 was kindly supplied by Dr. Steven Grant (VCU). PD184352, PD98059, NU1025, PJ34 and AG1478 were purchased from Calbiochem / EMD sciences (San Diego, CA). The validated siRNA molecules used knock down ATM (SI02663360; SI00299299; SI00604730) were from Qiagen (Germantown, MD). UCN-01 was purchased from Sigma-Aldrich (St. Louis MO). AZD7762 and AZD2281 were purchased from Axon Medchem (Groningen, Netherlands). UCN-01 was purchased from Sigma (St. Louis, MO). Obatoclax (GX15-070) was supplied by GeminX Pharmaceuticals (Malvern, PA).

Methods.

Culture and in vitro exposure of cells to drugs. Tumor cells for the studies in this manuscript were cultured at 37 ^{o}C (5% (v/v CO_2) *in vitro* using RPMI supplemented with 10% (v/v) fetal calf serum. *In vitro* Vehicle / UCN-01 / PD184352 / AZD7762 / PJ34 et al. treatment was from a 100 mM stock solution of each drug and the maximal concentration of Vehicle (DMSO) in media was 0.02% (v/v).

Cell treatments, SDS-PAGE and Western blot analysis. For in vitro analyses of short-term apoptosis effects, cells were treated with Vehicle / drugs or their combination for the indicated times. Cells for colony formation assays were plated at 250-4000 cells per well in sextupilcate and for *in vitro* assays 14 hours after plating were

Molecular Pharmacology Fast Forward. Published on August 9, 2010 as DOI: 10.1124/mol.110.067199
This article has not been copyedited and formatted. The final version may differ from this version.

treated with the individual or the drug combination(s) at a fixed increasing dose ratio according to the Method of T-C Chou and P Talalay, for 48h followed by drug removal. Ten-14 days after exposure or tumor isolation, plates were washed in PBS, fixed with methanol and stained with a filtered solution of crystal violet (5% w/v). After washing with tap water, the colonies were counted both manually (by eye) and digitally using a ColCount™ plate reader (Oxford Optronics, Oxford, England). Data presented is the arithmetic mean (± SEM) from both counting methods from multiple studies. Colony formation was defined as a colony of 50 cells or greater.

For SDS PAGE and immunoblotting, cells were plated at 5 x 10^5 cells / cm^2 and treated with therapeutic drugs at the indicated concentrations and after the indicated time of treatment, lysed with whole-cell lysis buffer (0.5 M Tris-HCl, pH 6.8, 2% SDS, 10% glycerol, 1% β-mercaptoethanol, 0.02% bromophenol blue), and the samples were boiled for 30 min. The boiled samples were loaded onto 10-14% SDS-PAGE and electrophoresis was run overnight. Proteins were electrophoretically transferred on to 0.22 μm nitrocellulose, and immunoblotted with various primary antibodies against different proteins. All immunoblots were visualized by use of an Odyssey Infra Red Imaging System.

Short-term cell viability assays after drug exposure. Cells were isolated at the indicated times in the Figure by trypsinization, and either subjected to trypan blue cell viability assay by counting in a light microscope or fixed to slides, and stained using a commercially available Diff Quick (Geimsa) assay kit.

Recombinant adenoviral vectors; infection in vitro. We generated and purchased previously noted recombinant adenoviruses to express constitutively activated MEK1 or AKT proteins and mitochondrial protective protein BCL-XL (Vector Biolabs, Philadelphia, PA). Unless otherwise stated, cells were infected with these adenoviruses at an approximate multiplicity of infection (m.o.i.) of 50. As noted above, cells were further incubated for 24 h to ensure adequate expression of transduced gene products prior to drug exposures.

Molecular Pharmacology Fast Forward. Published on August 9, 2010 as DOI: 10.1124/mol.110.067199
This article has not been copyedited and formatted. The final version may differ from this version.

siRNA transfection in vitro. Approximately 10 nM of a defined pre-validated siRNA (Ambion technologies) was diluted into 50 µl growth media lacking FBS and pen-strep. Based on the Manufacturer's instructions, an appropriate amount of Lipofectamine 2000 reagent (usually 1 µl) (Invitrogen, Carlsbad, CA) was diluted into a separate vial containing media with lacking FBS or pen-strep. The two solutions were incubated separately at room temperature for 5 min, then mixed together (vortexed) and incubated at room temperature for 30 min. The mixture was added to each well (slide or 12-well plate) containing an appropriate amount (~ 0.5 ml) of pen-strep- and FBS-free medium. Cells were incubated for 2-4 h at 37 deg C with gentle rocking. Media was then replaced with 1 ml of 1x pen-strep and FBS containing media.

Data analysis. Comparison of the effects between various in vitro drug treatments was performed following ANOVA using the Student's t test. Differences with a p-value of < 0.05 were considered statistically significant. Experiments shown are the means of multiple individual points from multiple studies (± SEM). Median dose effect isobologram colony formation analyses to determine synergism of drug interaction were performed according to the Methods of T-C Chou and P Talalay using the Calcusyn program for Windows (BIOSOFT, Cambridge, UK). Cells were treated with agents at an escalating fixed concentration drug dose. A indicates synergy of interaction between the two drugs; a combination index of ~ 1.00 indicates an additive interaction; a CI value of > 1.00 indicates antagonism of action between the agents.

Molecular Pharmacology Fast Forward. Published on August 9, 2010 as DOI: 10.1124/mol.110.067199
This article has not been copyedited and formatted. The final version may differ from this version.

Results.

Previously we have published that MEK1/2 inhibitors interact with UCN-01 in a synergistic manner to kill mammary tumor cells in vitro and in vivo (Hamed et al, 2008). To prove or refute whether UCN-01 and a chemically unrelated CHK1 inhibitor AZD7762, were mediating their ERK1/2 activating effects via inhibition of CHK1, we made use of a plasmid to express dominant negative CHK1. Expression of a dominant negative CHK1 protein in MCF7 cells enhanced basal levels of ERK1/2 phosphorylation within 24h and blunted the ability of UCN-01 or AZD7762 to stimulate ERK1/2 phosphorylation (Figure 1A).

UCN-01 was shown previously in malignant blood tumor cells to increase the phosphorylation of histone H2AX, indicative of DNA damage (Dai et al, 2008). Based on this observation, we determined whether another marker of the DNA damage response in tumor cells, PARP1 ADP ribosylation, could be visualized. Treatment of MCF7 breast cancer cells with either UCN-01 or AZD7762 increased PARP1 ADP ribosylation as judged using the anti-poly ADP ribose 10H antibody (Figure 1B). Of note, increased ERK1/2 phosphorylation correlated with elevated PARP1 (10H) reactivity. Co-exposure of cells to the PARP inhibitor PJ34 blocked CHK1 inhibitor –induced PARP1 activation and PARP1 ADP ribosylation. To confirm our findings using a molecular approach, we knocked down expression of PARP1. Knock down of PARP1 expression in breast cancer cells significantly reduced AZD7762 –induced activation of ERK1/2 (Figure 1C). Thus CHK1 inhibitor –induced ERK1/2 activation requires functional expression of PARP1.

In breast cancer cells UCN-01 and AZD7762 rapidly increased H2AX phosphorylation (Figures 2A and 2B). Inhibition of PARP1, either by use of PJ34 or by knock down of PARP1 expression, significantly reduced the induction of H2AX phosphorylation by the CHK1 inhibitors. In other model systems phosphorylation of H2AX has been shown to be mediated by the ataxia telangiectasia mutated (ATM) protein and PARP1 plays a key role in permitting ATM activation. Knock down of ATM expression prevented UCN-01 or AZD7762 from increasing H2AX phosphorylation (Figure 2C). Of note, both CHK1 inhibitors promoted a compensatory increase in CHK1 phosphorylation, which was also ATM dependent. Collectively, the data in Figures 1 and 2

Molecular Pharmacology Fast Forward. Published on August 9, 2010 as DOI: 10.1124/mol.110.067199
This article has not been copyedited and formatted. The final version may differ from this version.

demonstrates that CHK1 inhibitor mediated phosphorylation of both ERK1/2 and H2AX requires PARP1 function and that phosphorylation of H2AX after CHK1 inhibitor exposure requires expression of ATM.

We next explored the survival of PARP1 inhibited cells after CHK1 inhibitor treatment. Inhibition of PARP1 promoted CHK1 inhibitor lethality in a range of breast cancer cells (Figure 3A). Very similar data were obtained in pancreatic cancer cells (Figure 3B). In agreement with data using short term viability assays, median dose effect colony formation assays, as judged by combination index (CI) values of less than 1.00 demonstrated a synergy of drug interaction in killing tumor cells (Tables 1 and 2). PARP1 inhibitors are presently generating a significant level of clinical interest and we determined whether other more clinically relevant PARP1 inhibitors recapitulated the lethal effects of PJ34 or siRNA knock down of PARP1. The clinically relevant PARP1 inhibitors ABT888, NU1025 and AZD2281 enhanced the lethality of UCN-01 and of AZD7762 in breast cancer cells (Figure 3C). Similar data were obtained in other breast cancer cells (Figure 3D). As CHK1 inhibitor – induced ATM activation was PARP1 dependent, we determined the impact of inhibiting ATM function on drug combination lethality. Knock down of ATM expression significantly enhanced the lethality of PARP1 inhibitor + CHK1 inhibitor lethality, suggesting that in the absence of PARP1 + CHK1 signaling, the compensatory activation of ATM is a protective signal (Figure 3E). Similar data were obtained when a clinically relevant ATM inhibitor was used instead of siRNA knock down (Figure 3F). As manipulation of PARP1 / CHK1 function was leading to a DNA damage response in tumor cells, and inhibition of ATM further enhanced this effect, we next determined whether drug exposure enhanced tumor cell radiosensitivity. In both short-term and long-term colony assays inhibition of PARP1 + CHK1 function enhanced the toxic effects of exposure to ionizing radiation (Figure 3G).

In Figures 1 and 2 we noted that loss of PARP1 function suppressed CHK1 inhibitor –induced activation of ERK1/2. Inhibition of CHK1 inhibitor –induced ERK1/2 activation using a MEK1/2 inhibitor enhanced CHK1 inhibitor toxicity, an effect that was blocked by over-expressing an activated form of MEK1 (Figure 4A). However, expression of a constitutively activated MEK1 protein only *partially* suppressed the toxicity of

Molecular Pharmacology Fast Forward. Published on August 9, 2010 as DOI: 10.1124/mol.110.067199
This article has not been copyedited and formatted. The final version may differ from this version.

PARP1 inhibitor + CHK1 inhibitor treatment (Figure 4B). Expression of an activated form of AKT significantly suppressed PARP1 inhibitor + CHK1 inhibitor lethality and combined expression of activated MEK1 and AKT proteins abolished drug toxicity (Figure 4C).

Based on the cell survival findings in prior Figures, including evidence that ERK1/2 signaling promoted MCL-1 and BCL-XL expression, we determined the apoptosis pathway(s) being induced by the combination of CHK1 and PARP1 inhibitors. Transformed mouse embryonic fibroblasts genetically deleted for BAX/BAK were resistant to drug combination lethality (Figure 5A). In contrast, cells that were deleted for the caspase 8 substrate BID or for BIM did not exhibit any reduction in drug lethality (Figure 5A, data not shown). Over-expression of BCL-2 family proteins has been shown to block CHK1 inhibitor + MEK1/2 inhibitor lethality (Grant and Dent, 2007). Over-expression of BCL-XL suppressed CHK1 inhibitor + PARP1 inhibitor lethality that was reversed by addition of a small molecule inhibitor of BCL-2 family proteins, HA14-1 (Figure 5B). Similar data to HA14-1 were obtained when a clinically relevant BCL-2 / BCL-XL / MCL-1 inhibitor Obatoclax (GX15-070) was used. Collectively, these findings demonstrate that CHK1 inhibitors synergize with PARP1 inhibition to kill multiple carcinoma cell types via the intrinsic apoptosis pathway.

Molecular Pharmacology Fast Forward. Published on August 9, 2010 as DOI: 10.1124/mol.110.067199
This article has not been copyedited and formatted. The final version may differ from this version.

Discussion

Previous studies by this group have argued that MEK1/2 inhibitors or farnesyltransferase inhibitors interact with the CHK1 inhibitor UCN-01 to promote tumor cell specific killing in a wide variety of malignancies including breast, prostate and multiple hematological cell types [reviewed in Grant and Dent, 2007]. The net output of the cytoprotective RAS - MEK1/2 - ERK1/2 pathway has previously been shown to be a critical determinant of tumor cell survival (reviewed in Riches et al, 2008). Furthermore, activation of this cascade has been observed as a compensatory response of tumor cells to various environmental stresses, including cytotoxic drugs. The present studies were initiated to determine in whether CHK1 inhibitors, which cause ERK1/2 activation and a DNA damage response, interact with inhibitors of PARP1; PARP1 is a protein that plays a key role in DNA repair and regulation of ERK1/2 signaling. Based on expression of a dominant negative CHK1 protein, UCN-01 and AZD7762 –induced activation of ERK1/2 was dependent upon inhibition of CHK1; furthermore, expression of dominant negative CHK1 enhanced basal levels of ERK1/2 phosphorylation arguing for a central regulatory role between CHK1 and the RAF-MEK-ERK1/2 pathway. Thus our findings argue that inhibition of CHK1 is essential, in part, for activation of ERK1/2 to occur by CHK1 inhibitors.

Suppression of CHK1 function has been shown to cause DNA damage in transformed cells as judged by increased H2AX phosphorylation. The damage-stimulated phosphorylation of H2AX has been associated with the actions of the ataxia telangiectasia mutated (ATM) protein (Riches et al, 2008). An additional hallmark of the cellular DNA damage response is activation of PARP1 (Rodon et al, 2009). PARP1 activation results in ADP ribosylation of multiple DNA repair complex proteins, transcription factors as well as PARP1 itself. As a result of this effect on multiple repair proteins, loss of PARP1 function promotes genomic instability and leads to hyper-activation of CHK1 with increased cell numbers in G2 phase (Lu et al, 2006). This is also of interest because other groups have postulated the chemotherapy sensitizing effect of CHK1 inhibitors is due to abrogation of the G2 checkpoint (Prudhomme, 2006). In our studies two chemically distinct CHK1 inhibitors rapidly promoted H2AX phosphorylation and increased PARP1 ADP ribosylation. Inhibition of PARP1 function blocked CHK1 inhibitor –induced H2AX phosphorylation, as well as blocking CHK1 inhibitor –

Molecular Pharmacology Fast Forward. Published on August 9, 2010 as DOI: 10.1124/mol.110.067199
This article has not been copyedited and formatted. The final version may differ from this version.

induced activation of ERK1/2. The inhibition of –induced H2AX phosphorylation by PARP inhibition is likely explained by the requirement ATM has for PARP1 function in being able to become activated following DNA damage and in our studies knock down of ATM blocked CHK1 inhibitor – induced H2AX phosphorylation (Haince et al, 2007). And of note, ATM / checkpoint pathway signaling has previously been linked in one of our prior studies to regulation of the ERK1/2 pathway (Golding et al, 2007).

Previously we presented evidence that inhibition of CHK1 –induced ERK1/2 activation further enhanced H2AX phosphorylation, indicative that loss of ERK1/2 signaling increased the amount of DNA damage being induced by the CHK1 inhibitor (Dai et al, 2008). This correlated with a subsequent profound induction of apoptosis. The present work demonstrated that inhibition of PARP1 blocked not only ERK1/2 activation but also blocked H2AX phosphorylation. However, despite blocking the apparent DNA damage signaling response, we found that PARP1 inhibitors significantly enhanced the lethality of CHK1 inhibitors. Based on the use of BAX/BAK -/- cells, as well as expression of BCL-XL, the induction of mitochondrial dysfunction was shown to play a primary role in the synergistic induction of cell killing following treatment of cells with a PARP1 inhibitor and CHK1 inhibitors. Of note, mammary carcinoma cells with very low basal levels of ERK1/2 activity and that are relatively non-invasive such as MCF7 were apparently as susceptible to being killed by exposure to PARP1 inhibitor and CHK1 inhibitors as were mammary carcinoma cells and pancreatic cancer cells with very high basal levels of ERK1/2 activity and that are highly invasive such as MDA-MB-231 and PANC-1. SV40 large T antigen transformed fibroblasts that are not tumorigenic in mice were also sensitive to the drug schedule, although in agreement with prior findings, we have found that multiple non-transformed / non-established cell types such as primary mammary epithelial cells and CD34+ stem cells are insensitive to being killed by the CHK1 inhibitor + PARP1 pathway inhibitor combined drug exposure regimen [unpublished observations]. Collectively, our data suggests that CHK1 function plays a key role in maintaining cell viability in transformed cells and does so, in part, by regulating ERK1/2 pathway signaling as part of a DNA damage response.

Over-expression of mitochondrial BCL-2 family members has been shown in many tumor cell systems to raise the apoptotic threshold of tumor cells (Lee and Gautschi, 2006; Cory and Adams, 2005; Konopleva et al, 2008). As the potentiation of CHK1 inhibitor lethality by PARP1 inhibition occurs primarily by promoting mitochondrial dysfunction, it would be assumed that over time, one of the mechanisms by which cells could survive this treatment will be a viability-selection based on increased expression of BCL-2 family members. With this general possibility in mind for multiple chemotherapeutic treatments, several drug companies have developed small molecule inhibitors of BCL-2, BCL-XL and MCL-1, including the drugs Gossypol, ABT-737 / ABT-263 and GX15-070 (Obatoclax) (Tse et al, 2008; Nguyen et al, 2007). In the present studies we noted that a commercially available inhibitor of BCL-2 and BCL-XL, HA14-1, significantly enhanced the lethality of the two drug (CHK1 inhibitor + PARP1 inhibitor) regimen. Prior studies have also shown that HA14-1 can overcome the protective effect of BCL-XL in cells treated with UCN-01 and PD184352 (Hamed et al, 2008). Furthermore, the clinically relevant BCL-2 inhibitor Obatoclax also enhanced (CHK1 inhibitor + PARP1 inhibitor) toxicity and overcame the protective effect of BCL-XL over-expression. Collectively, these findings demonstrate that the potentiation of CHK1 inhibitor lethality by PARP1 inhibitors can be profoundly enhanced by additional destabilization of mitochondrial function via inhibition of BCL-2 family member activity(ies).

In conclusion, inhibition of PARP1 blocks CHK1 inhibitor –induced activation of both the DNA damage response machinery and of ERK1/2. Studies beyond the scope of the present manuscript will be required to determine whether this drug combination alters tumor cell survival in vivo.

Molecular Pharmacology Fast Forward. Published on August 9, 2010 as DOI: 10.1124/mol.110.067199
This article has not been copyedited and formatted. The final version may differ from this version.

References.

Bucher N, Britten CD. G2 checkpoint abrogation and checkpoint kinase-1 targeting in the treatment of cancer. Br J Cancer. 2008; 98:523–528.

Cory S, Adams JM. Killing cancer cells by flipping the Bcl-2/Bax switch. Cancer Cell. 2005; 8:5-6.

Dai Y, Yu C, Singh V, Tang L, Wang Z, McInistry R, Dent P, Grant S. Pharmacological inhibitors of the mitogen-activated protein kinase (MAPK) kinase/MAPK cascade interact synergistically with UCN-01 to induce mitochondrial dysfunction and apoptosis in human leukemia cells. Cancer Res. 2001; 61:5106-15.

Dai Y, Landowski TH, Rosen ST, Dent P, Grant S. Combined treatment with the checkpoint abrogator UCN-01 and MEK1/2 inhibitors potently induces apoptosis in drug-sensitive and -resistant myeloma cells through an IL-6-independent mechanism. Blood. 2002; 100:3333-43.

Dai Y, Chen S, Pei XY, Almenara JA, Kramer LB, Venditti CA, Dent P, Grant S. Interruption of the Ras/MEK/ERK signaling cascade enhances Chk1 inhibitor-induced DNA damage in vitro and in vivo in human multiple myeloma cells. Blood. 2008; 112: 2439-49.

Dees EC, Baker SD, O'Reilly S, et al. A phase I and pharmacokinetic study of short infusions of UCN-01 in patients with refractory solid tumors. Clin Cancer Res 2005; 11:664–671.

Fuse E, Tanii H, Kurata N, et al. Unpredicted clinical pharmacology of UCN-01 caused by specific binding to human alpha1-acid glycoprotein. Cancer Res 1998; 58: 3248-3253.

Fuse E, Kuwabara T, Sparreboom A, Sausville EA, Figg WD. Review of UCN-01 development: a lesson in the importance of clinical pharmacology. J Clin Pharmacol 2005; 45:394–403.

Golding SE, Rosenberg E, Neill S, Dent P, Povirk LF, Valerie K. Extracellular signal-related kinase positively regulates ataxia telangiectasia mutated, homologous recombination repair, and the DNA damage response. Cancer Res. 2007; 67: 1046-53.

Grant S, Dent P. Simultaneous interruption of signal transduction and cell cycle regulatory pathways: implications for new approaches to the treatment of childhood leukemias. Curr Drug Targets. 2007; 8:751-9.

Graves PR, Yu L, Schwarz JK, et al, The Chk1 protein kinase and the Cdc25C regulatory pathways are targets of the anticancer agent UCN-01. J Biol Chem 2000; 275: 5600-5605.

Grazia Graziani G, Szabó C. Clinical perspectives of PARP inhibitors Pharmacological Research 2005; 52: 109-118.

Hagan MP, Yacoub A, Dent P. Radiation-induced PARP activation is enhanced through EGFR-ERK signaling. J Cell Biochem. 2007; 101: 1384-93.

Hagenauer B, Maier-Salamon A, Thalhammer T, Zollner P, Senderowicz A, Jager W. Metabolism of UCN-01 in isolated perfused rat liver: role of Mrp2 in the biliary excretion of glucuronides. Oncol Rep 2004; 11: 1069-1075.

Haince JF , K ozlov S, Da wson V L, Da wson T M, He ndzel M J, L avin MF, Poi rier GG . A taxia telangiectasia mutated (ATM) signaling network is modulated by a novel poly (ADP-ribose)-dependent pathway in the early response to DNA-damaging agents. J Biol Chem. 2007; 282:16441-53.

Hamed H, Hawkins W, Mitchell C, et al. Transient exposure of carcinoma cells to RAS/MEK inhibitors and UCN-01 causes cell death in vitro and in vivo. Mol Cancer Ther. 2008; 7: 616-29.

Hawkins W, Mitchell C, McKinstry R, et al. Transient exposure of mammary tumors to PD184352 and UCN-01 cau ses t umor c ell d eath i n vivo a nd p rolonged s uppression of t umor regr owth. C ancer B iol Ther. 2005; 4: 1275-84.

Hotte SJ, Oza A, Winquist EW, et al. Phase I trial of UCN-01 in combination with topotecan in patients with advanced solid cancers: a Princess Margaret Hospital Phase II Consortium study. Ann Oncol 2006; 17:334-40.

Komander D , Kular GS , Bain J , Elliott M , Alessi DR , Van Aalten DM . Structural basis for UCN-01 (7-hydroxystaurosporine) s pecificity an d P DK1 (3-phosphoinositide-dependent protein kinase-1) inhibition. Biochem J. 2003; 375 :255-262.

Konopleva M , W att J , C ontractor R, et a l. Mechanisms of an tileukemic a ctivity of t he n ovel B cl-2 homology domain-3 mimetic GX15-070 (obatoclax). Cancer Res. 2008; 68: 3413-20.

Lee D, Gautschi O. Clinical development of SRC tyrosine kinase inhibitors in lung cancer. Clin Lung Cancer. 2006; 7: 381-4.

Lu HR, Wang X, Wang Y. A stronger DNA damage-induced G2 checkpoint due to over-activated CHK1 in the absence of PARP-1. Cell Cycle. 2006; 5: 2364-70.

McCabe N, Turner NC, Lord CJ, et al. Deficiency in the repair of DNA damage by homologous recombination and sensitivity to poly (ADP-ribose) polymerase inhibition. Cancer Res. 2006; 66: 8109-15.

McKinstry R, Qiao L, Yacoub A, et al. Pharmacologic inhibitors of the mitogen activated protein kinase cascade interact synergistically with UCN-01 to induce mitochondrial dysfunction and apoptosis in mammary and prostate carcinoma cells. Cancer Biology and Therapy 2002; 1: 241-251.

Mow BM, Blajeski AL, Chandra J, Kaufmann SH. Apoptosis and the response to anticancer therapy. Curr Opin Oncol 2001; 13: 453-462.

Nguyen M, Marcellus RC, Roulston A, et al. Small molecule obatoclax (GX15-070) antagonizes MCL-1 and overcomes MCL-1-mediated resistance to apoptosis. Proc Natl Acad Sci U S A. 2007; 104: 19512-7.

Pei, X-Y, Dai Y, Chen S, Bodie WW, Kramer, LB, Dent P, Grant S. The MEK1/2 inhibitor AZD6244 (ARRY-142886) interacts synergistically with the novel Chk1 inhibitor AZD7762 to induce apoptosis in human multiple myeloma cells. Proc. Am. Assoc. Cancer Res. 2008; Abstract LB-103.

Peng C-Y, Graves PR, Thoma RS, et al, Mitotic and G_2 checkpoint control: regulation of 14-3-3 protein binding by phosphorylation of Cdc25C on serine-216. Science 1997; 277: 1501-1505.

Perez RP, Lewis LD, Beelen AP, et al. Modulation of cell cycle progression in human tumors: a pharmacokinetic and tumor molecular pharmacodynamic study of cisplatin plus the Chk1 inhibitor UCN-01 (NSC 638850). Clin Cancer Res. 2006; 12:7079-85.

Prudhomme M. Novel checkpoint 1 inhibitors. Recent Patents Anticancer Drug Discov. 2006; 1: 55-68.

Quénet D, El Ramy R, Schreiber V, Dantzer F. The role of poly(ADP-ribosyl)ation in epigenetic events. Int J Biochem Cell Biol. 2009; 41:60-5.

Riches LC, Lynch AM, Gooderham NJ. Early events in the mammalian response to DNA double-strand breaks. Mutagenesis. 2008; 23: 331-9.

Rodon J, Iniesta MD, Papadopoulos K. Development of PARP inhibitors in oncology. Expert Opin Investig Drugs. 2009; 18: 31-43.

Sausville EA, Lush RD, Headlee D, et al. Clinical pharmacology of UCN-01: initial observations and comparison to preclinical models. Cancer Chemother Pharmacol 1998; 42 Suppl: S54-59.

Schreiber V, Dantzer F, Ame JC, de Murcia G. Poly (ADP-ribose): Novel functions for an old molecule. Nat Rev Mol Cell Biol 2006; **7**: 517-528.

Schreiber V, Ame JC, Dolle P, et al. Poly(ADP-ribose) polymerase-2 (PARP-2) is required for efficient base excision DNA repair in association with PARP-1 and XRCC1. J Biol Chem 2002; 277: 23028-23036.

Spina Purrello V, Cormaci G, Denaro L, et al. Effect of growth factors on nuclear and mitochondrial ADP-ribosylation processes during astroglial cell development and aging in culture. Mech Ageing Dev. 2002; 123: 511-20.

Syljuåsen RG, Sorensen CS, Hansen LT, et al. Inhibition of human Chk1 causes increased initiation of DNA replication, phosphorylation of ATR targets, and DNA breakage. Mol Cell Biol. 2005; 25:3553–3562.

Tse C, Shoemaker A R, Adickes J, et al. ABT-263: a potent and orally bioavailable Bcl-2 family inhibitor. Cancer Res. 2008; 68: 3421-8.

Molecular Pharmacology Fast Forward. Published on August 9, 2010 as DOI: 10.1124/mol.110.067199
This article has not been copyedited and formatted. The final version may differ from this version.

Footnotes.

This work was funded from PHS grants (R01-DK52825; P01-CA104177; R01-CA108325; R01-CA150214), Department of Defense Awards (DAMD17-03-1-0262 and W81XWH-10-1-0009) and by The Jim Valvano "Jimmy V" Foundation and The Goodwin Foundation. PD is the holder of the Universal Inc. Professorship in Signal Transduction Research.

Molecular Pharmacology Fast Forward. Published on August 9, 2010 as DOI: 10.1124/mol.110.067199
This article has not been copyedited and formatted. The final version may differ from this version.

Figure Legends

Figure 1. Inhibition of CHK1 enhances ERK1/2 activation in a PARP-1 dependent fashion. Panel A. MCF7 cells were transfected with either an empty vector control plasmid or a plasmid to express dominant negative CHK1 (dnCHK1). Twenty four hours after transfection, cells were treated with vehicle (VEH, DMSO), UCN-01 (100 nM) or AZD7762 (50 nM). Cells were isolated at the indicated time points and subjected to SDS PAGE followed by immunoblotting to determine the phosphorylation of ERK1/2 (P-ERK1/2) or the expression of GAPDH. Data are from a representative of 2 separate studies. **Panel B.** MCF7 cells were treated with vehicle (VEH, DMSO) or the PARP-1 inhibitor PJ34 (3 μM) followed 30 min later by CHK1 inhibitors either UCN-01 (100 nM) or AZD7762 (50 nM). Cells were isolated 0-6h after CHK1 inhibitor addition, as indicated in the panel. Cell lysates were subjected to SDS PAGE followed by immunoblotting to determine the phosphorylation of ERK1/2 (P-ERK1/2), the ADP ribosylation of PARP-1 (10H antibody) or the expression of GAPDH. Data are from a representative of 3 separate studies. **Panel C.** MCF7 cells were transfected with either a scrambled non-specific siRNA (siSCR, 20 nM) or and siRNA to knock down expression of PARP-1. Twenty four h after transfection, cells were treated with AZD7762 (50 nM). Cells were isolated at the indicated time points and subjected to SDS PAGE followed by immunoblotting to determine the phosphorylation of ERK1/2 (P-ERK1/2), the expression of PARP-1 or the expression of GAPDH. Data are from a representative of 2 separate studies.

Figure 2. PARP-1 is essential for CHK1 inhibitor –induced phosphorylation of histone H2AX. Panel A. MCF7 cells were treated with vehicle (VEH, DMSO) or the PARP-1 inhibitor PJ34 (3 μM) followed 30 min later by CHK1 inhibitors either UCN-01 (100 nM) or AZD7762 (50 nM). Cells were isolated 0-6h after CHK1 inhibitor addition, as indicated in the panel. Cell lysates were subjected to SDS PAGE followed by immunoblotting to determine the phosphorylation of H2AX or the expression of GAPDH. Data are from a representative of 3 separate studies. **Panel B.** MCF7 cells were transfected with either a scrambled non-specific siRNA (siSCR, 20 nM) or and siRNA to know down expression of PARP-1. Twenty four h after transfection,

cells were treated with UCN-01 (100 nM) or AZD7762 (50 nM). Cells were isolated at the indicated time points and subjected to SDS PAGE followed by immunoblotting to determine the phosphorylation of H2AX, the expression of PARP-1 or the expression of GAPDH. Data are from a representative of 2 separate studies. **Panel C.** MCF7 cells were transfected with non-specific siRNA control (siSCR) or an siRNA to knock down ATM (siATM). Twenty four h after transfection cells were treated with vehicle (VEH, DMSO) or by CHK1 inhibitors either UCN-01 (100 nM) or AZD7762 (50 nM). Cells were isolated 3h after CHK1 inhibitor addition, as indicated in the panel. Cell lysates were subjected to SDS PAGE followed by immunoblotting to determine the phosphorylation of H2AX / CHK1 or the expression of GAPDH, ATM, CHK1 and H2AX. Data are from a representative of 3 separate studies.

Figure 3. PARP-1 inhibition enhances the toxicity of CHK1 inhibitors in transformed cells. Panel A. Breast cancer cells were plated in triplicate and treated with vehicle (VEH, DMSO), PJ34 (3 μM), UCN-01 (50 nM) or AZD7762 (25 nM). Cells were isolated 48h after exposure and viability determined using trypan blue exclusion. Data for each assay is the mean of all data points from three studies ± SEM. **Panel B.** MCF7 breast cancer and PANC-1 and MiaPaca2 pancreatic cancer cells were plated in triplicate and treated with vehicle (VEH, DMSO), PJ34 (3 μM), UCN-01 (50 nM) or AZD7762 (25 nM). Cells were isolated 48h after exposure and viability determined using trypan blue exclusion. Data for each assay is the mean of all data points from three studies ± SEM. **Panel C.** MCF7 cells were plated in triplicate and treated with vehicle (VEH, DMSO), NU1025 (10 μM), AZD2281 (0.5 μM), ABT888 (1.0 μM) and / or AZD7762 (25 nM) or UCN-01 (50 nM). Cells were isolated 48h after exposure and viability determined using trypan blue exclusion. Data for each assay is the mean of all data points from three studies ± SEM. **Panel D.** SKBR3 and BT474 cells were plated in triplicate and treated with vehicle (VEH, DMSO), NU1025 (10 μM), and / or AZD7762 (25 nM). Cells were isolated 48h after exposure and viability determined using trypan blue exclusion. Data for each assay is the mean of all data points from three studies ± SEM. **Panel E.** MCF7 cells were transfected with non-specific siRNA control (siSCR) or an siRNA to knock down ATM (siATM). Twenty four h after transfection cells were

Molecular Pharmacology Fast Forward. Published on August 9, 2010 as DOI: 10.1124/mol.110.067199
This article has not been copyedited and formatted. The final version may differ from this version.

treated with vehicle (VEH, DMSO) and/or by AZD7762 (25 nM) or UCN-01 (50 nM). Cells were isolated 48h after exposure and viability determined using trypan blue exclusion. Data for each assay is the mean of all data points from three studies ± SEM. **Panel F.** MCF7 cells were plated in triplicate and treated with vehicle (VEH, DMSO), AZD2281 (0.5 μM), AZD7762 (25 nM) or AZD2281 + AZD7762 in combination. Thirty minutes after exposure cells are treated with vehicle (DMSO) or with increasing concentrations of the ATM inhibitor KU55933 (1-10 μM). Cells were isolated 48h after exposure and viability determined using trypan blue exclusion. Data for each assay is the mean of all data points from three studies ± SEM. **Panel G.** *LEFT*: MCF7 cells were plated and treated with vehicle (VEH, DMSO) or the PARP-1 inhibitor PJ34 (3 μM) followed 30 min later by CHK1 inhibitor AZD7762 (25 nM). Cells were irradiated (4 Gy) and for short term viability assays 48 h after exposure and viability determined using trypan blue exclusion. *RIGHT*: MCF7 cells were plated in sextuplicate as single cells and 12h after plating cells were treated with vehicle (VEH, DMSO) or the PARP-1 inhibitor PJ34 (3 μM) followed 30 min later by CHK1 inhibitors either UCN-01 (50 nM) or AZD7762 (25 nM). Cells were irradiated 30 min after drug additions. Forty eight hours after drug exposure, the media was changed and cells cultured in drug free media for an additional 10-14 days (n = 2 +/- SEM).

Figure 4. Inhibition of CHK1 inhibitor –induced ERK1/2 activation is not the sole molecular mechanism of drug interaction. Panel A. MCF7 cells were infected in triplicate at an m.o.i. of 50 with either an empty vector adenovirus (CMV) or with an adenovirus to express constitutively activated MEK1 EE. Twenty four h after infection cells were treated with vehicle (VEH, DMSO), PD98059 (25 μM), or UCN-01 (50 nM) as indicated. Cells were isolated 48h after exposure and viability determined using trypan blue exclusion. Data for each assay is the mean of all data points from three studies ± SEM. **Panel B.** MCF7 cells were infected in triplicate at an m.o.i. of 50 with either an empty vector adenovirus (CMV) or with an adenovirus to express constitutively activated MEK1 EE. Twenty four h after infection cells were treated as indicated with vehicle (VEH, DMSO), PJ34 (3 μM), UCN-01 (50 nM) or AZD7762 (25 nM). Cells were isolated 48h after exposure and viability determined using trypan blue exclusion. Data for each assay is the mean of all data points from

three studies ± SEM. **Panel C.** MCF7 cells were infected in triplicate at an m.o.i. of 50 with either an empty vector adenovirus (CMV) or with adenoviruses to express constitutively activated MEK1 EE and/or constitutively activated AKT. Twenty four h after infection cells were treated as indicated with vehicle (VEH, DMSO), PJ34 (3 μM) and/or AZD7762 (25 nM) as indicated. Cells were isolated 48 h after exposure and viability determined using trypan blue exclusion. Data for each assay is the mean of all data points from three studies ± SEM.

Figure 5. Loss of BAX/BAK function abolishes the toxic interaction between CHK1 inhibitors and PARP-1 inhibitors; cell killing is potentiated by inhibitors of BCL-2/BCL-XL function. Panel A. Transformed mouse embryonic fibroblasts, MEF (wild type, WT; deleted for BAX and BAK, BAX/BAK -/-; deleted for BID, BID -/-) were plated in triplicate and treated with vehicle (VEH, DMSO), PJ34 (3 μM), UCN-01 (50 nM) or AZD7762 (25 nM). Cells were isolated 48 h after exposure and viability determined using trypan blue exclusion. Data for each assay is the mean of all data points from three studies ± SEM. **Panel B.** PANC-1 and MCF7 cells were infected with either an empty vector adenovirus (CMV) or with an adenovirus to express BCL-XL. Twenty four h after infection cells were pre-treated for 30 min with vehicle (VEH, DMSO) or HA14-1 (10 μM) and then treated as indicated with vehicle (VEH, DMSO) or PJ34 (3 μM) and UCN-01 (50 nM). Cells were isolated 48h after exposure and viability determined in triplicate using trypan blue exclusion. Data for each assay is the mean of all data points from two studies ± SEM. **Panel C.** MCF7 cells were infected with either an empty vector adenovirus (CMV) or with an adenovirus to express BCL-XL. Twenty four h after infection cells were pre-treated for 30 min with vehicle (VEH, DMSO) or Obatoclax (GX15-070, 50 nM) and then treated as indicated with vehicle (VEH, DMSO) or PJ34 (3 μM) and UCN-01 (50 nM). Cells were isolated 48h after exposure and viability determined in triplicate using trypan blue exclusion. Data for each assay is the mean of all data points from two studies ± SEM. * $p < 0.05$ less than corresponding value in empty vector virus infected cells; # $p < 0.05$ greater than corresponding value in empty vector infected cells not treated with Obatoclax; $ greater than corresponding value in BCL-XL infected cells treated with Obatoclax.

Molecular Pharmacology Fast Forward. Published on August 9, 2010 as DOI: 10.1124/mol.110.067199
This article has not been copyedited and formatted. The final version may differ from this version.

Table 1. CHK1 inhibitors synergize with PARP1 inhibitors to kill pancreatic carcinoma cells. PANC-1 (pancreatic) and MiaPaca2 (pancreatic) carcinoma cells plated as single cells (250-2000 cells/well) in sextuplicate and 12h after this plating the infected cells were treated with vehicle (VEH, DMSO), the PARP1 inhibitor PJ34 (0.75-3.0 μM), the CHK1 inhibitors UCN-01 (22.5-37.5 nM) or AZD7762 (6.25-25.0 nM) or the combinations of the PARP1 and CHK1 inhibitor drugs combined, as indicated at a fixed concentration ratio to perform median dose effect analyses for the determination of synergy. Forty eight hours after drug exposure, the media was changed and cells cultured in drug free media for an additional 10-14 days. Cells were fixed, stained with crystal violet and colonies of > 50 cells / colony counted. Colony formation data were entered into the Calcusyn program and combination index (CI) values determined. A CI value of less than 1.00 indicates synergy.

Panc1

AZD7762 (nM)	PJ34 (μM)	Fa	CI
6.25	0.75	0.26	0.40
12.5	1.50	0.39	0.48
25.0	3.00	0.62	0.43

UCN01 (nM)	PJ34 (μM)	Fa	CI
12.5	0.75	0.27	0.41
25.0	1.50	0.42	0.44
50.0	3.00	0.54	0.58

MiaPaca2

AZD7762 (nM)	PJ34 (μM)	Fa	CI
6.25	0.75	0.38	0.51
12.5	1.50	0.45	0.68
25.0	3.00	0.68	0.62

UCN01 (nM)	PJ34 (μM)	Fa	CI
12.5	0.75	0.37	0.45
25.0	1.50	0.44	0.68
50.0	3.00	0.74	0.40

Molecular Pharmacology Fast Forward. Published on August 9, 2010 as DOI: 10.1124/mol.110.067199
This article has not been copyedited and formatted. The final version may differ from this version.

Table 2. CHK1 inhibitors synergize with PARP1 inhibitors to kill mammary carcinoma cells. MCF7 carcinoma cells plated as single cells (250-2000 cells/well) in sextuplicate and 12h after this plating the infected cells were treated with vehicle (VEH, DMSO), the PARP1 inhibitor PJ34 (0.75-3.0 μM), the CHK1 inhibitors UCN-01 (22.5-37.5 nM) or AZD7762 (6.25-25.0 nM) or the combinations of the PARP1 and CHK1 inhibitor drugs combined, as indicated at a fixed concentration ratio to perform median dose effect analyses for the determination of synergy. Forty eight hours after drug exposure, the media was changed and cells cultured in drug free media for an additional 10-14 days. Cells were fixed, stained with crystal violet and colonies of > 50 cells / colony counted. Colony formation data were entered into the Calcusyn program and combination index (CI) values determined. A CI value of less than 1.00 indicates synergy.

MCF7

AZD7762 (nM)	PJ34 (M)	Fa	CI
6.25	0.75	0.16	0.49
12.5	1.50	0.33	0.52
25.0	3.00	0.51	0.54
UCN01 (nM)	PJ34 (M)	Fa	CI
12.5	0.75	0.17	0.53
25.0	1.50	0.32	0.54
50.0	3.00	0.43	0.47

Molecular Pharmacology Fast Forward. Published on August 9, 2010 as DOI: 10.1124/mol.110.067199
This article has not been copyedited and formatted. The final version may differ from this version.

Figure 1A

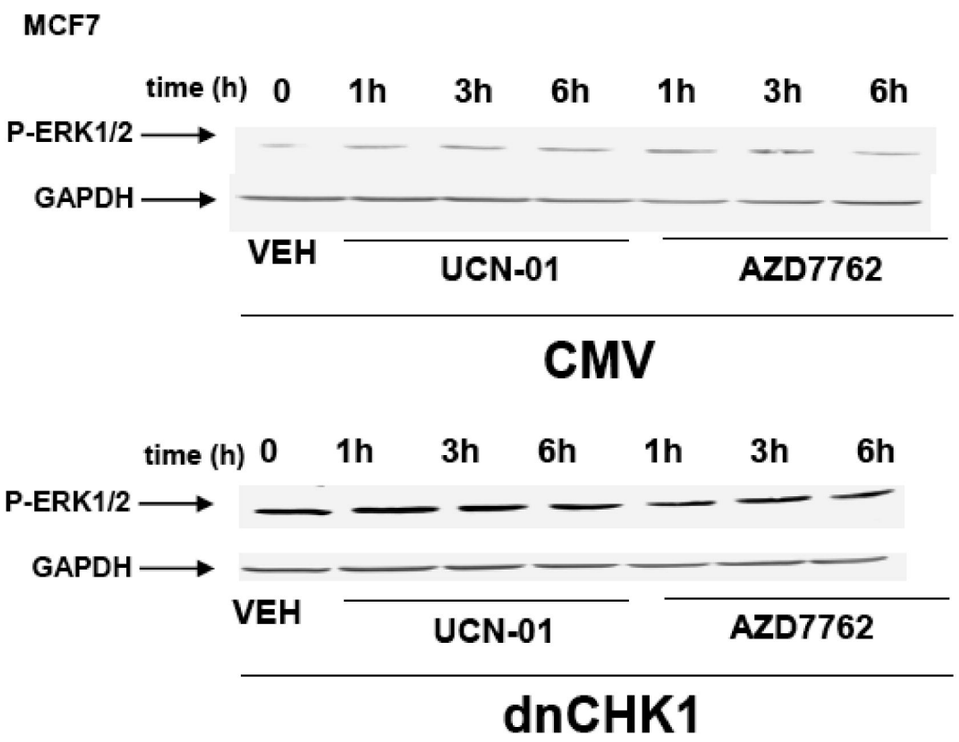

Figure 1B

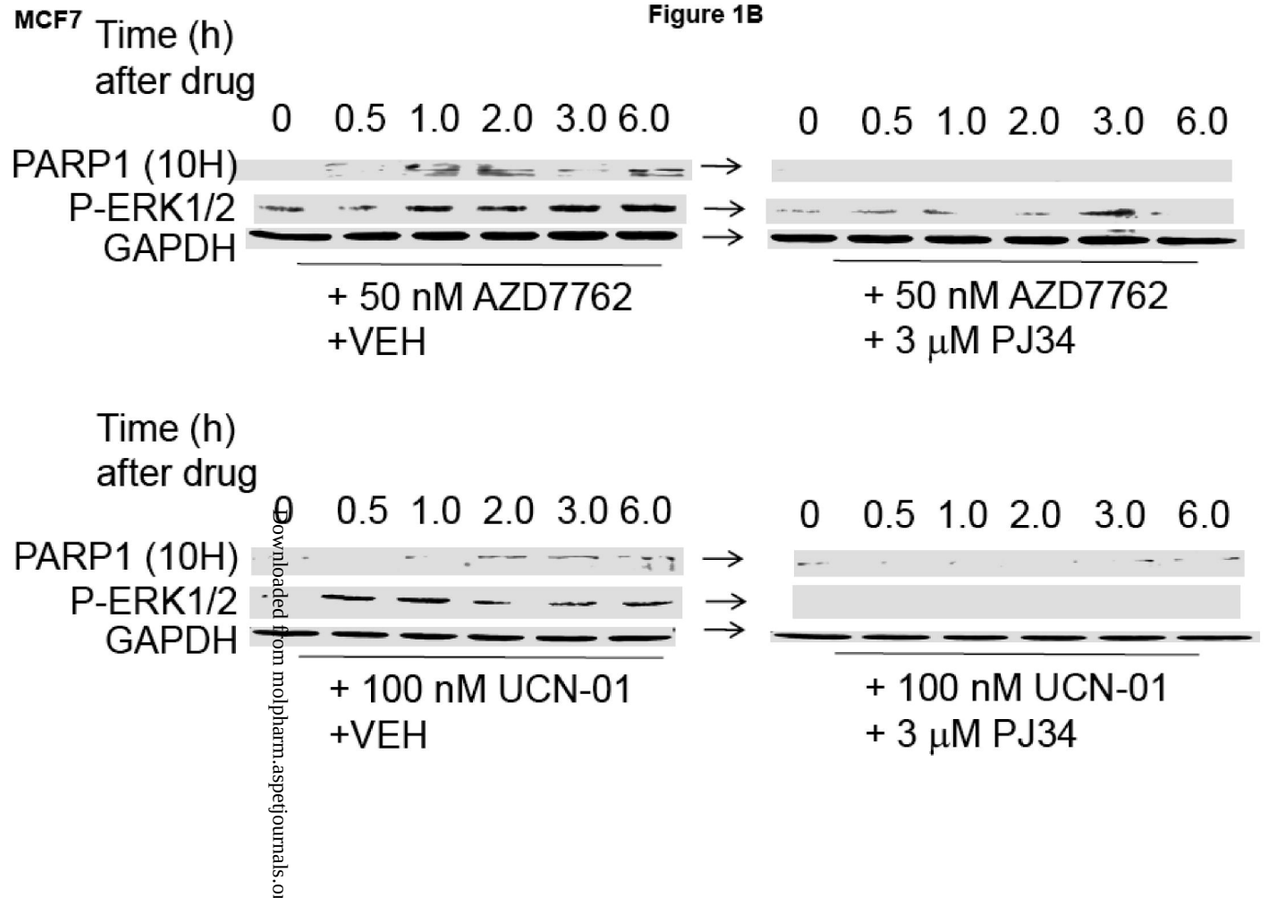

Figure 1C

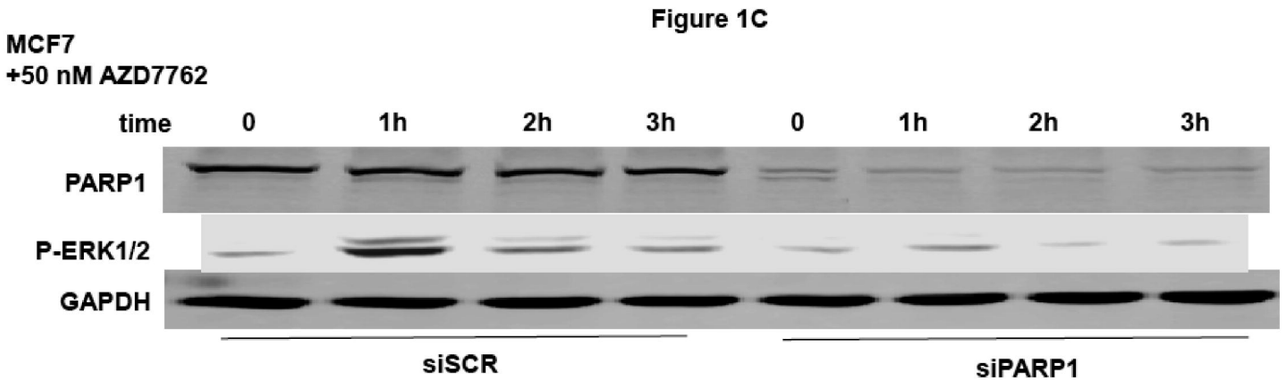

Molecular Pharmacology Fast Forward. Published on August 9, 2010 as DOI: 10.1124/mol.110.067199
This article has not been copyedited and formatted. The final version may differ from this version.

Figure 2A

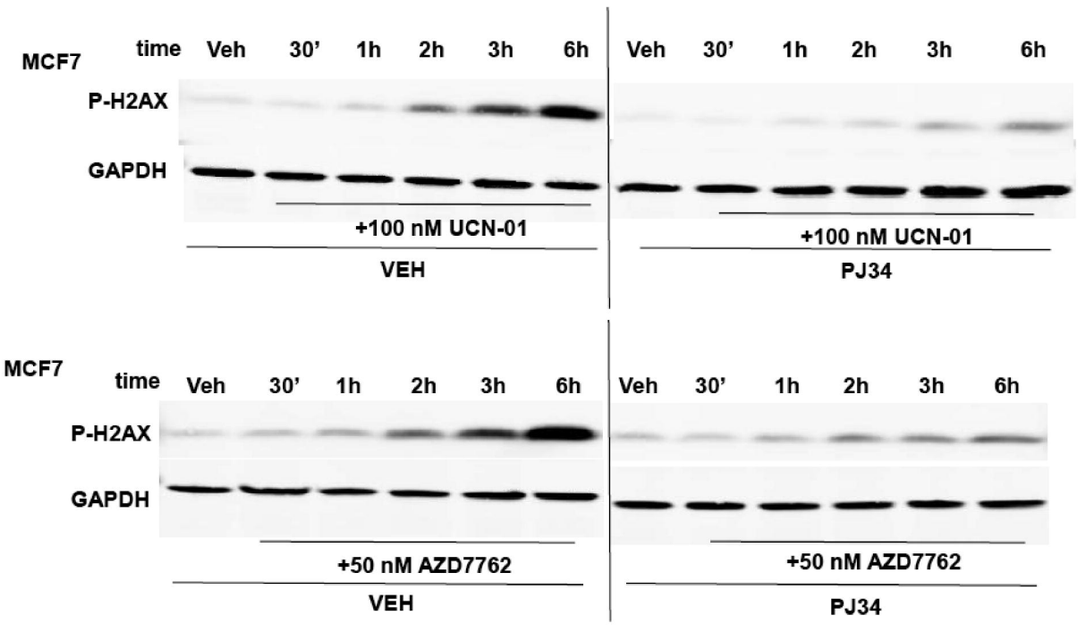

Figure 2B

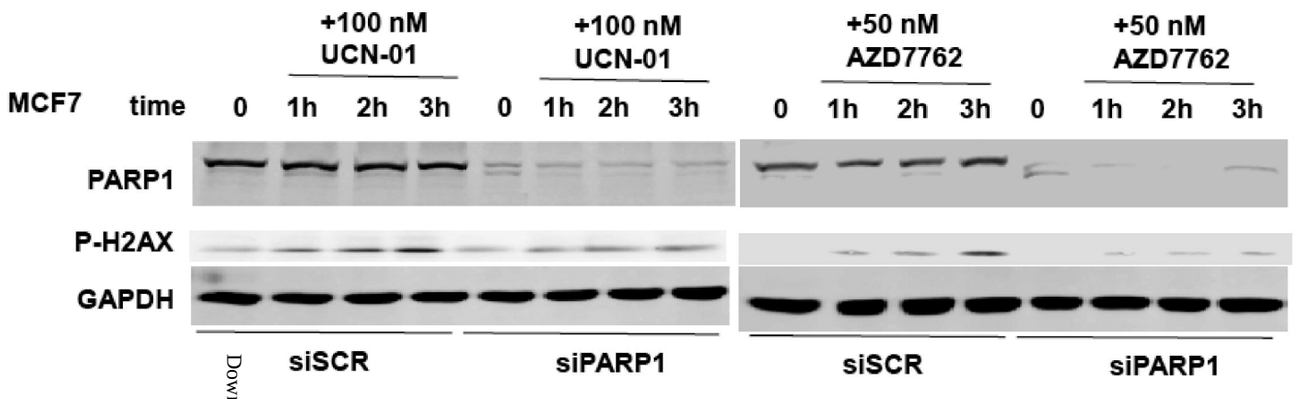

Figure 2C

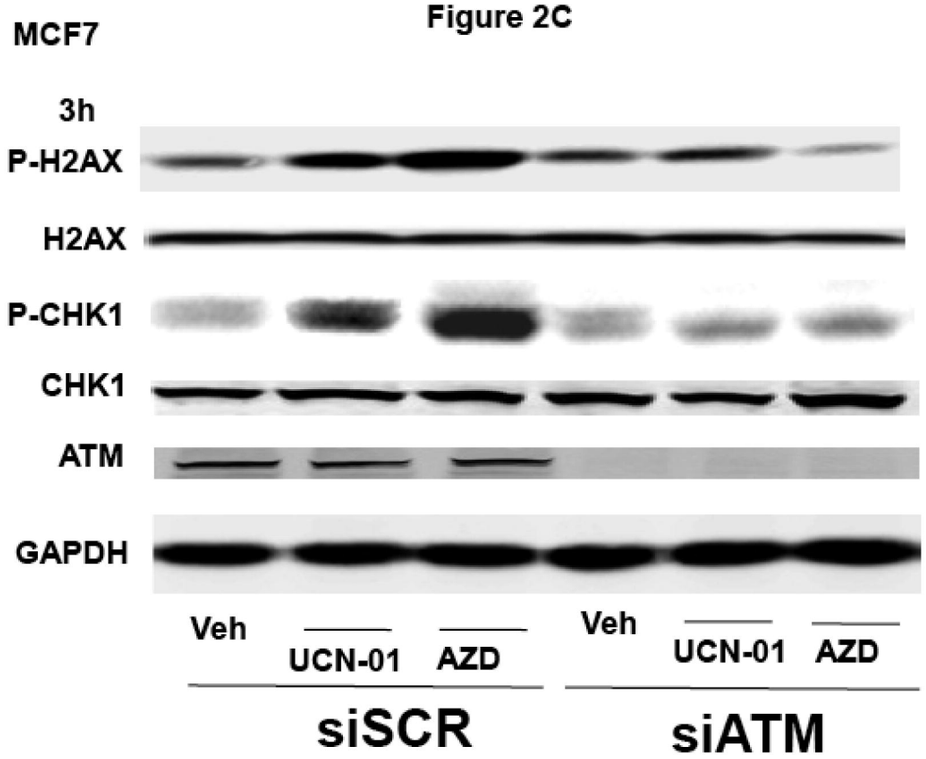

Molecular Pharmacology Fast Forward. Published on August 9, 2010 as DOI: 10.1124/mol.110.067199
This article has not been copyedited and formatted. The final version may differ from this version.

Figure 3A

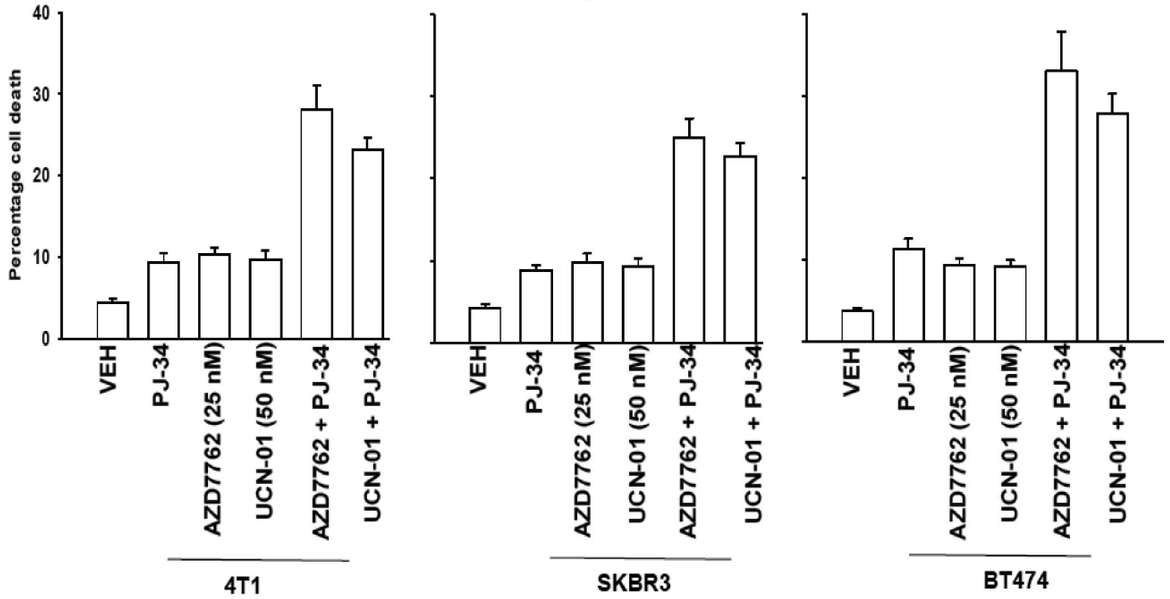

Figure 3B

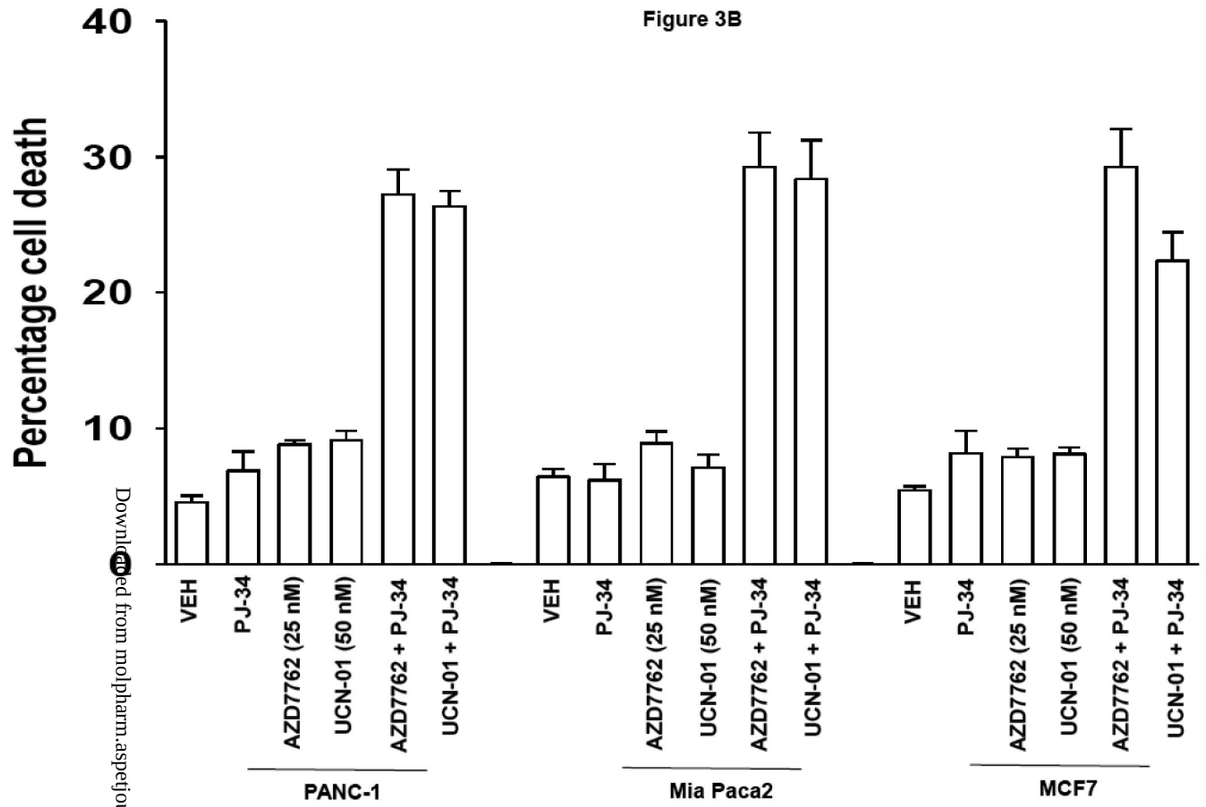

Figure 3C

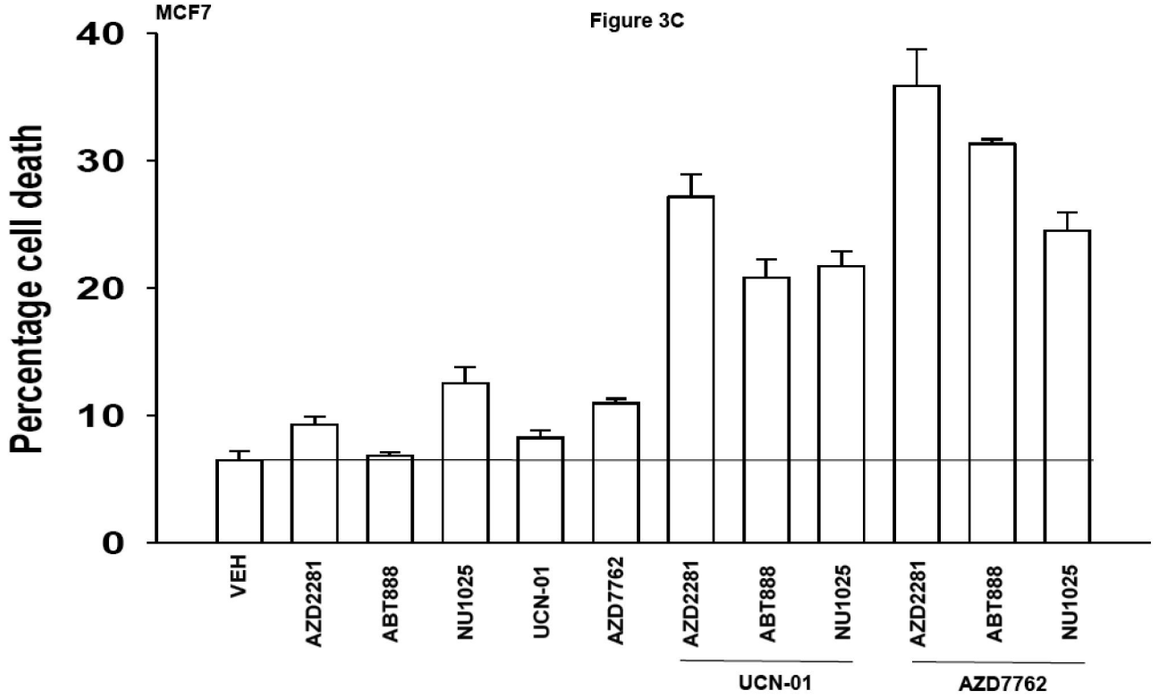

Figure 3D

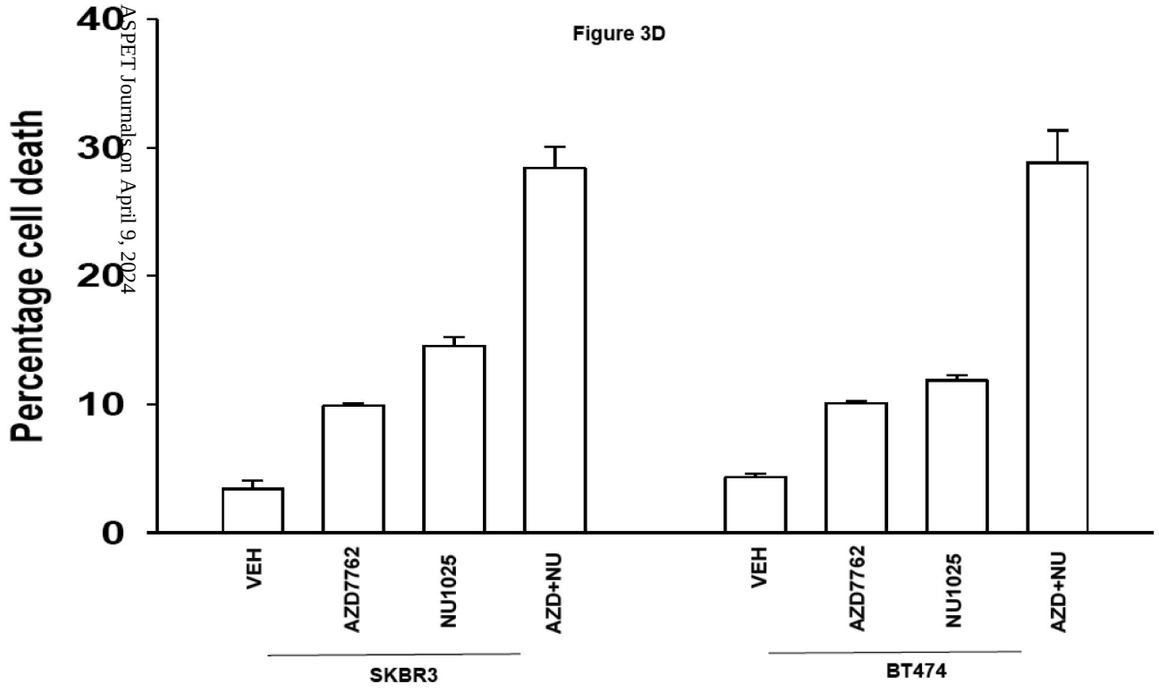

Molecular Pharmacology Fast Forward. Published on August 9, 2010 as DOI: 10.1124/mol.110.067199
This article has not been copyedited and formatted. The final version may differ from this version.

Figure 3E

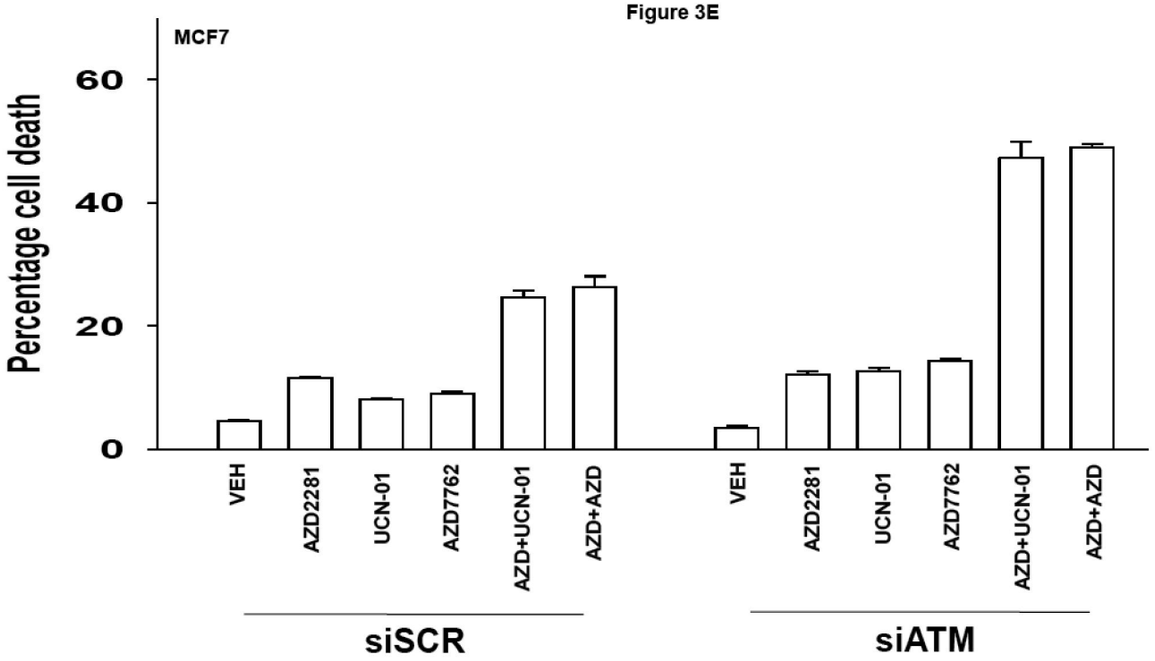

Figure 3F

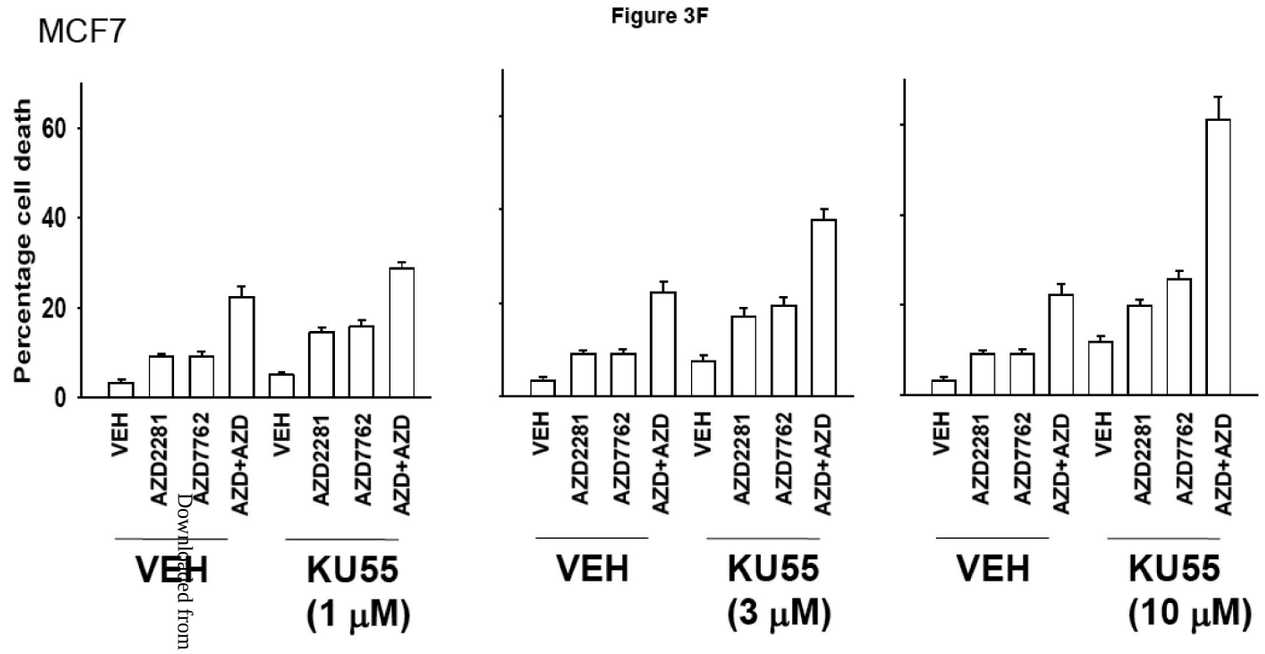

Figure 3G

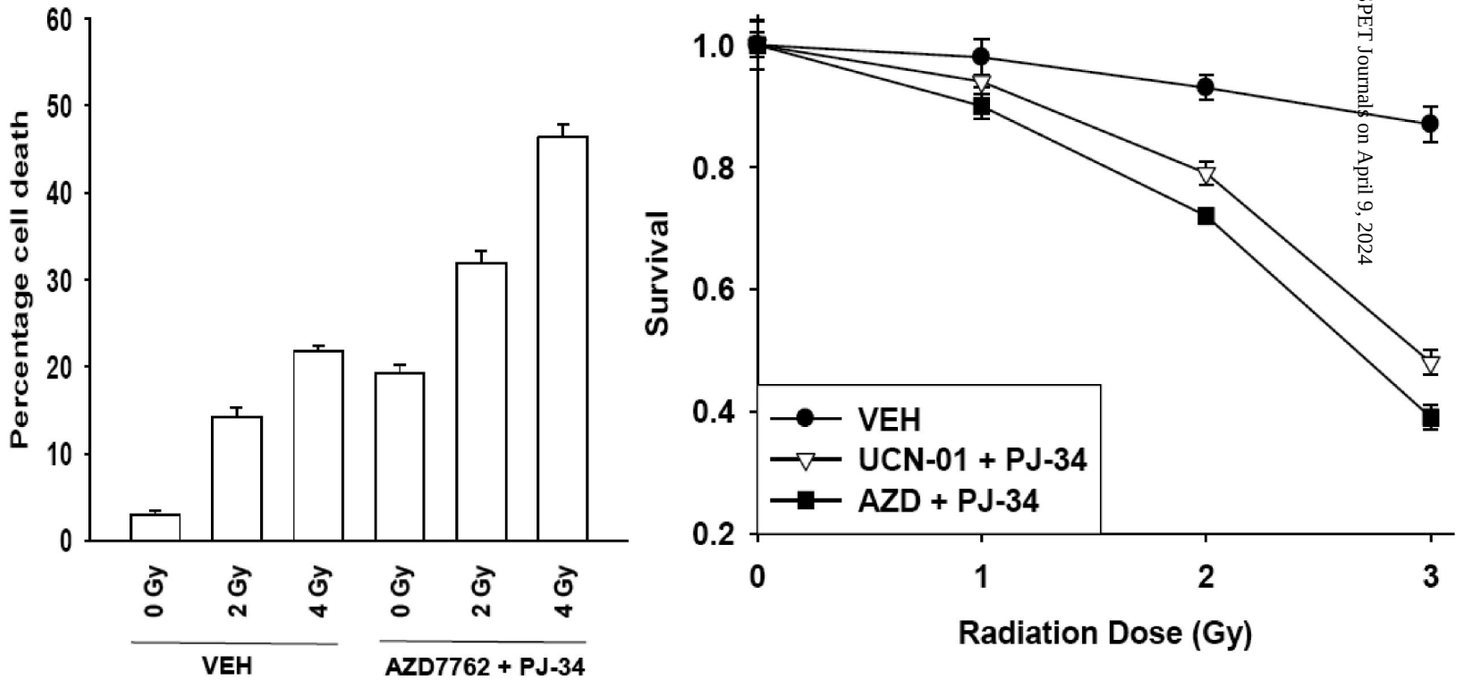

Molecular Pharmacology Fast Forward. Published on August 9, 2010 as DOI: 10.1124/mol.110.067199
This article has not been copyedited and formatted. The final version may differ from this version.

Figure 4A

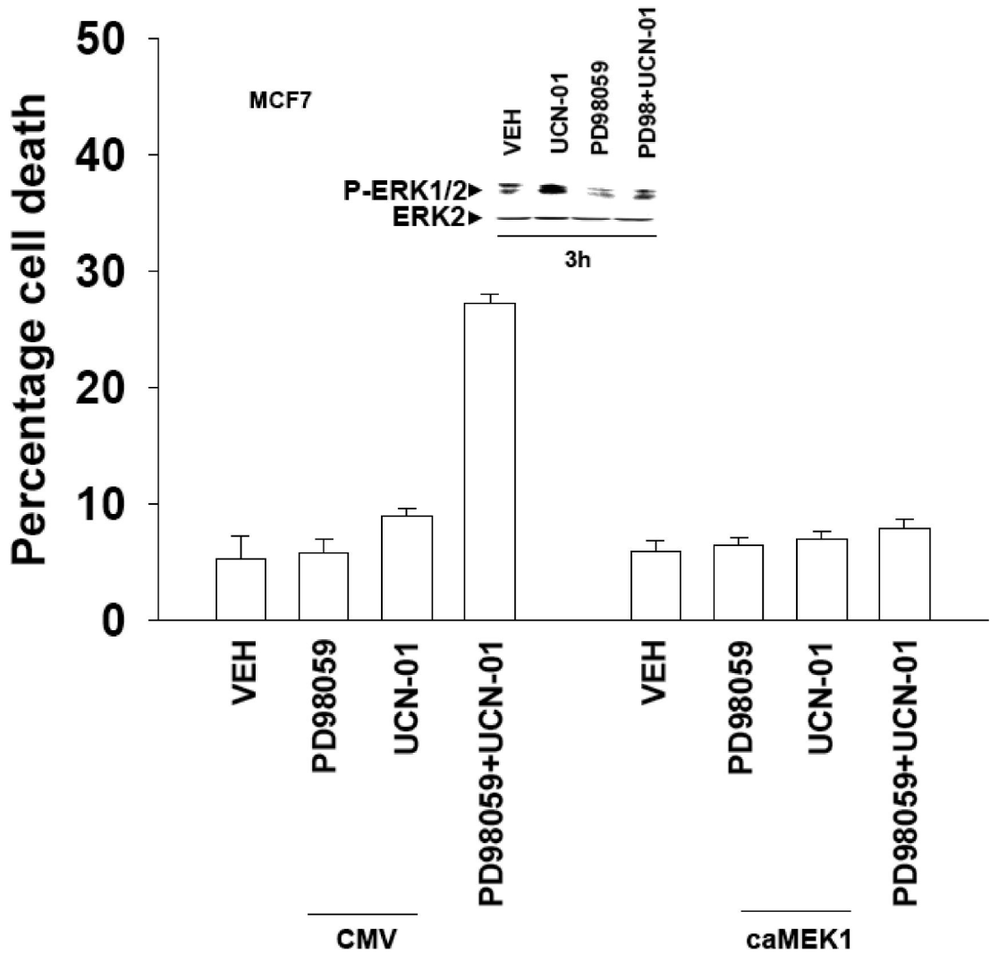

Figure 4B

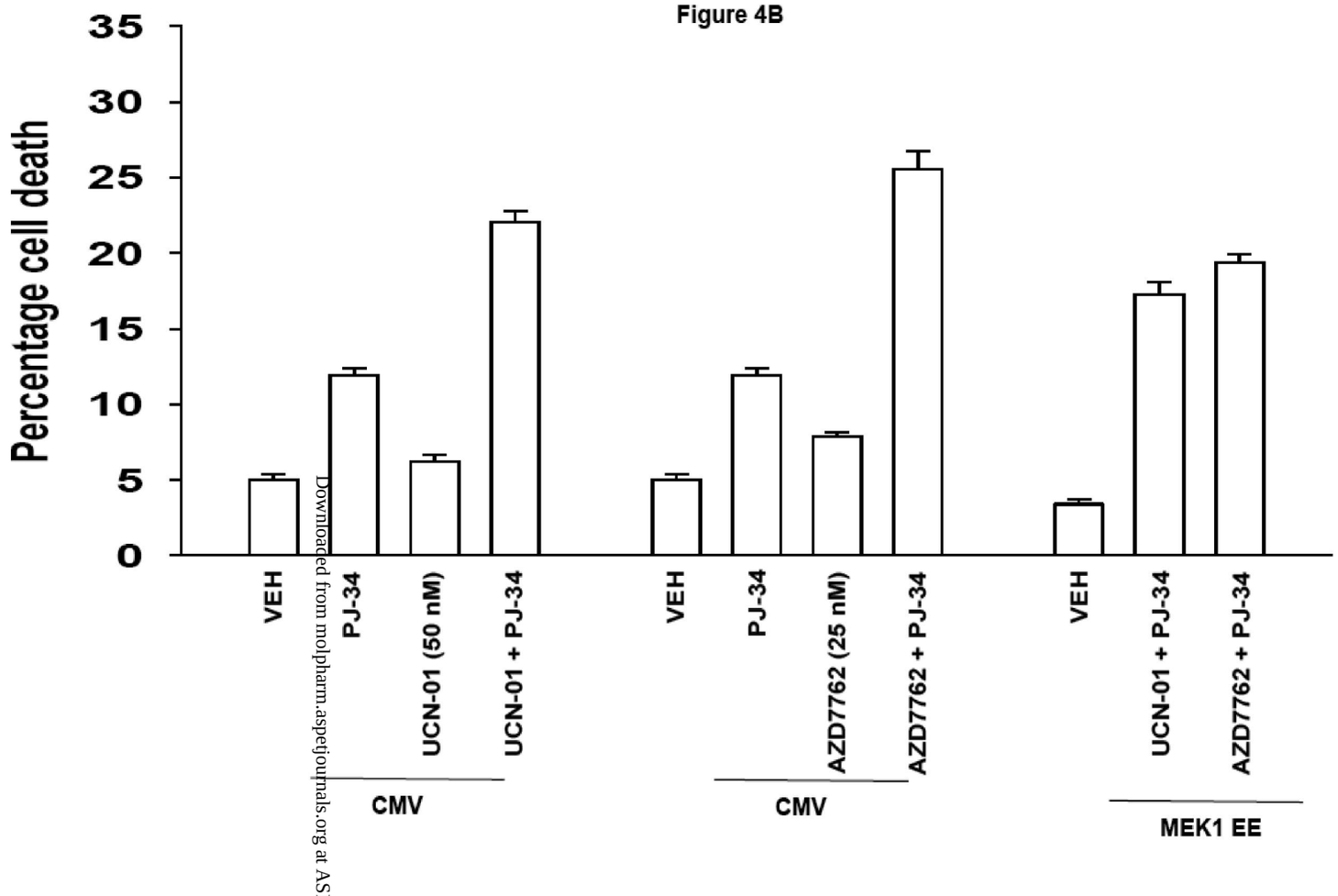

Figure 4C

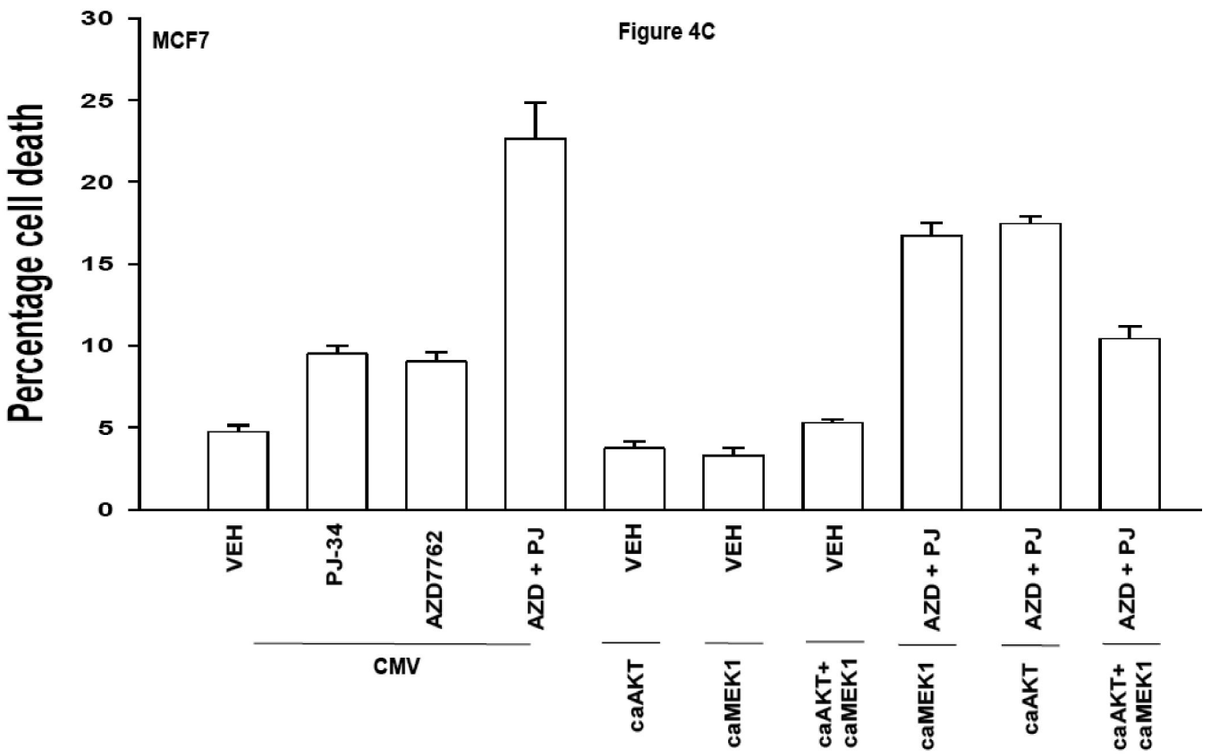

Molecular Pharmacology Fast Forward. Published on August 9, 2010 as DOI: 10.1124/mol.110.067199
This article has not been copyedited and formatted. The final version may differ from this version.